Low-Speed Performance Enhancement using Localized Active Flow Control

Simulations, Scaling and Design of Localized Active Flow Control on the Common Research Model (4/4)

Arvin Shmilovich, The Boeing Company
Matthew Stauffer, The Boeing Company
Rene Woszidlo, The Boeing Company
Paul Vijgen, The Boeing Company

April 27, 2022

Table of Contents

List of Figures

Nomenclature

Parameters

α	Angle of attack
AR	Aspect ratio of actuator at the throat
A_{throat}	Total nozzle throat area
C_L	Airplane lift coefficient
$C_{L,max}$	Maximum lift coefficient
C_p	Pressure coefficient
C_q	mass flow coefficient, $m_j/(\rho_\infty u_\infty A_{ref})$
h	Height of actuator at the throat
L/D	Lift-to-drag ratio
M	Mach number
P	Pressure
P_{0in}	Total pressure at the actuator inlet
$P_{0\infty}$	Freestream total pressure
PR	Total pressure ratio, $P_{0in}/P_{0\infty}$
PT	Normalized total pressure, $P_0/P_{0\infty}$
Re	Reynolds number based on mean aerodynamic chord
U_∞	Freestream velocity
w	Width of actuator at the throat

Subscripts

0	Stagnation
∞	Freestream

Acronyms

AFC	Active Flow Control
AoA	Angle of Attack
CAD	Computer Aided Design
CD	Convergent-divergent
CFD	Computational Fluid Dynamics
CRM-HL	High Lift Common Research Model
NASA	National Aeronautics and Space Administration
OML	Outer mold line
RefG	Reference geometry

Executive Summary

This report is dedicated to the application of localized AFC on the NASA CRM-HL wind tunnel model, with focus on the aileron application discussed in the CFD study (final report document #2). The experience developed for the Reference Aircraft guided the implementation on the CRM model. CFD evaluations are performed on a representative high-lift configuration, for a set of aileron deflections, and at relevant flow conditions. Alternative flow control actuator layouts are proposed and design consideration for practical integration into the existing CRM-HL model are set forth. The CFD simulations indicate that the aerodynamic performance improvements due to AFC obtained for the CRM-HL are consistent with those achieved for the Reference Aircraft. The observed changes in L/D are smaller than for the Reference Aircraft because the CRM has a higher leading edge sweep angle and a different relative aileron size. Conceptual design studies confirmed that the integration of an AFC equipped aileron into the existing wind tunnel model is feasible.

1 Introduction

Documents #2 and #3 of the final report package [1,2] focus on the analysis of a relevant reference aircraft in order to extract realistic metrics for aerodynamic performance benefits and aircraft level performance net-benefits due to AFC. However, the aerodynamic assessment of three AFC concepts is solely based on numerical simulations which warrants the need for experimental validation of AFC effects. One suitable aircraft model is the Common Research Model (CRM). NASA and other researchers have utilized this geometry for numerous studies. NASA already has a 10% scale, CRM-HL model that has been tested extensively in the NASA LaRC 14- by 22-Foot Subsonic Tunnel (14x22), including the use of AFC for replacing the complex high-lift system with an AFC augmented simple flap configuration [3,4]. Initially, NASA planned to test AFC concepts on this model in the Fall of 2021, which has been delayed to January of 2023 due to the global pandemic. In order to prepare for and support this test as much as possible, the Boeing team conducted a numerical study dedicated to the CRM-HL geometry. Based on the literature review summarized in document #1 [5] and the CFD results reported in document #2 [1], the team decided to focus on the AFC concept over a deflected aileron. The expected aerodynamic deltas are more suitable for a wind tunnel test and the integration of this AFC concept into NASA's existing wind tunnel model is more realistic than other AFC concepts. However, the current CRM-HL model does not have an aileron defined, which was one of the first tasks to complete (Section 2.1). Furthermore, the CRM is a much different aircraft geometry than the one considered as a reference geometry for AFC integration and performance assessment. The CRM is more representative of a long haul commercial aircraft whereas the reference geometry used in this project is more akin to a short/medium haul commercial aircraft. Therefore, the relative scaling of baseline performance metrics and AFC parameters needed to be placed in perspective (Section 2.2). Last, the required modifications to the existing wind tunnel model had to be evaluated. The Boeing team reviewed the current wind tunnel model design and developed suitable concepts to modify the existing model with minimal effort to insert an AFC equipped, deflectable aileron (Section 4).

2 Geometry Definition for the CRM-HL Model

A two-step process is employed for developing the geometry for the AFC-equipped aileron of the CRM-HL wind tunnel model. The first step focuses on the wing planform for the relevant high-lift conditions, including the definition of the aileron itself, which had not been available previously (Section 2.1). The second step involves the development of the AFC layout, guided by the findings from the CFD portion of the study on the Reference Aircraft (final report document #2 [1]). In addition, Section 2.2 addresses the relative scaling of aerodynamic performance metrics and AFC variables between the CRM-HL and the Reference Aircraft.

2.1 Wing Planform and Aileron Definition

For the aileron AFC application, a set of modifications are needed for the current CRM-HL wind tunnel model. First, the aileron itself has to be defined. Figure 1 provides a planform view of the wing and relevant coordinates of aerodynamic surfaces. The aileron hingeline is defined with its planar full-scale coordinates. This aileron represents a conventional size and is similar to the Reference Aircraft, scaled to the CRM-HL planform. In addition, the aileron coordinates of the 10% scale wind tunnel model are visualized in an isometric view in Figure 2. Planes parallel and perpendicular to the freestream mark the start and end of the aileron hingeline. The planform normal direction is defined as the center of the local airfoil height along the aileron hingeline (Figure 3). This information fully defines the aileron location and size. The outer mold line (OML) of the aileron is retained and extracted from the OML of the wing without an aileron.

Note that the choice for the hingeline normal direction (i.e., half the local airfoil thickness) is preliminary and requires a final determination by the CRM focals. NASA's final design for the model modification should be carefully with the Boeing team to ensure consistency with the CRM community.

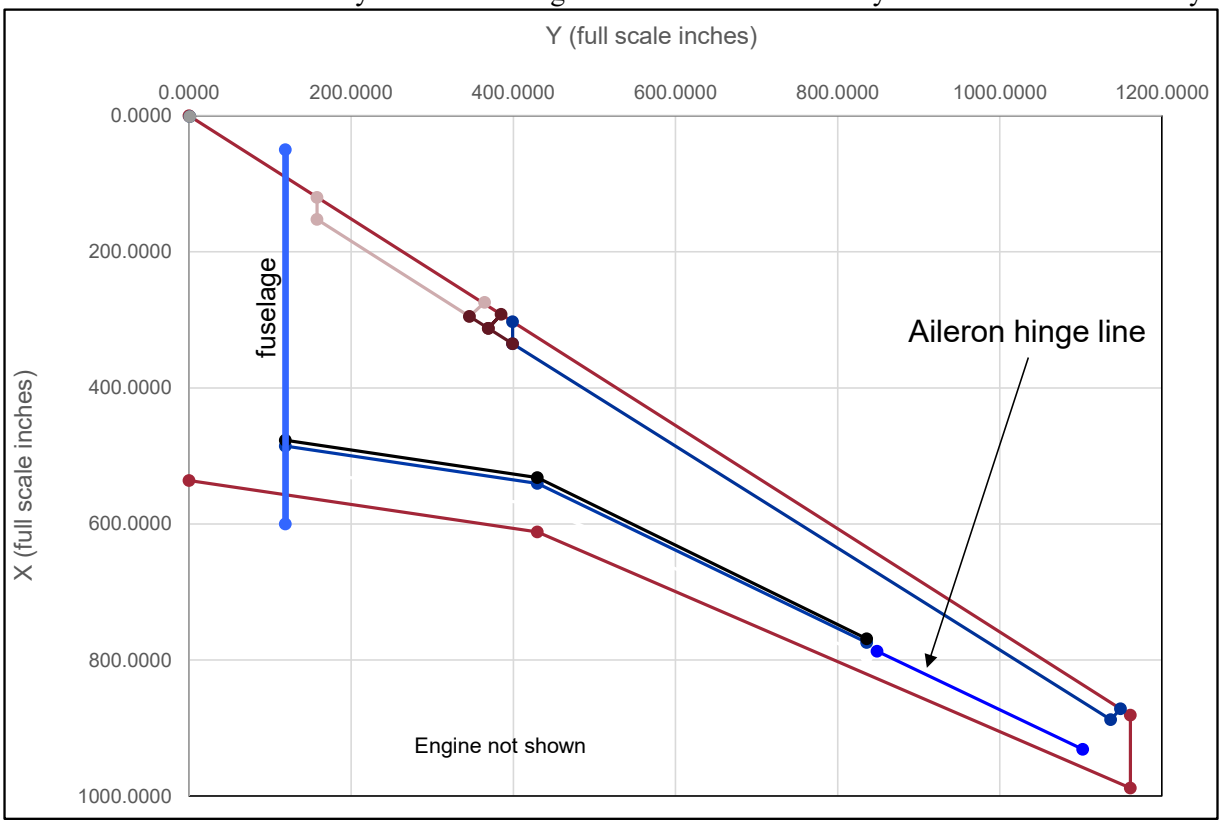

Figure 1 – Coordinates of aileron on full-scale CRM-HL geometry.

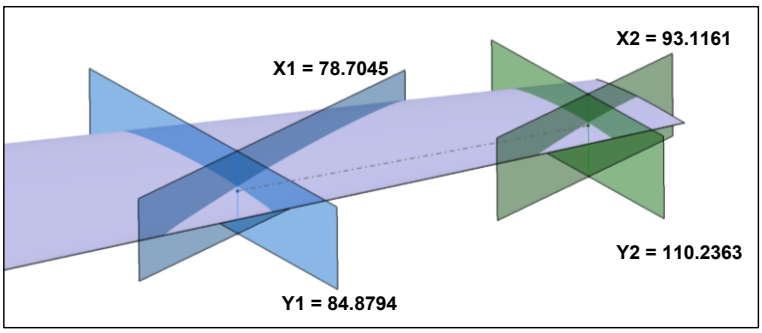

Figure 2 – Aileron hingeline coordinates (in inches) for CRM-HL wind tunnel model with planes normal and perpendicular to the freestream direction.

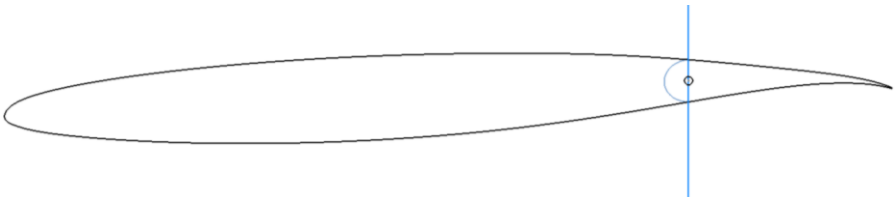

Figure 3 – Hingeline located at half the local airfoil height (preliminary choice).

In addition to defining the aileron, the CRM-HL geometry also had to be prepared for numerical simulations in the takeoff configuration. For takeoff, the slats are sealed and the flaps deflected to appropriate angles. Furthermore, a fixed peninsula between the flap and the aileron was inserted with representative caps that were scaled from reference commercial aircraft. Details of the sealed slat, aileron surface and peninsula are visualized in Figure 4. Additional perspective views are offered in Figure 5. For CFD purposes, the transition between main wing OML and aileron OML at various deflection angles was created manually in the grid generation process, similar to the approach used in the Reference Aircraft.

Note that all definitions, CAD files, CFD files and additional documentation for the baseline CRM-HL configuration at takeoff and with an aileron were provided to NASA as part of project deliverable 3.

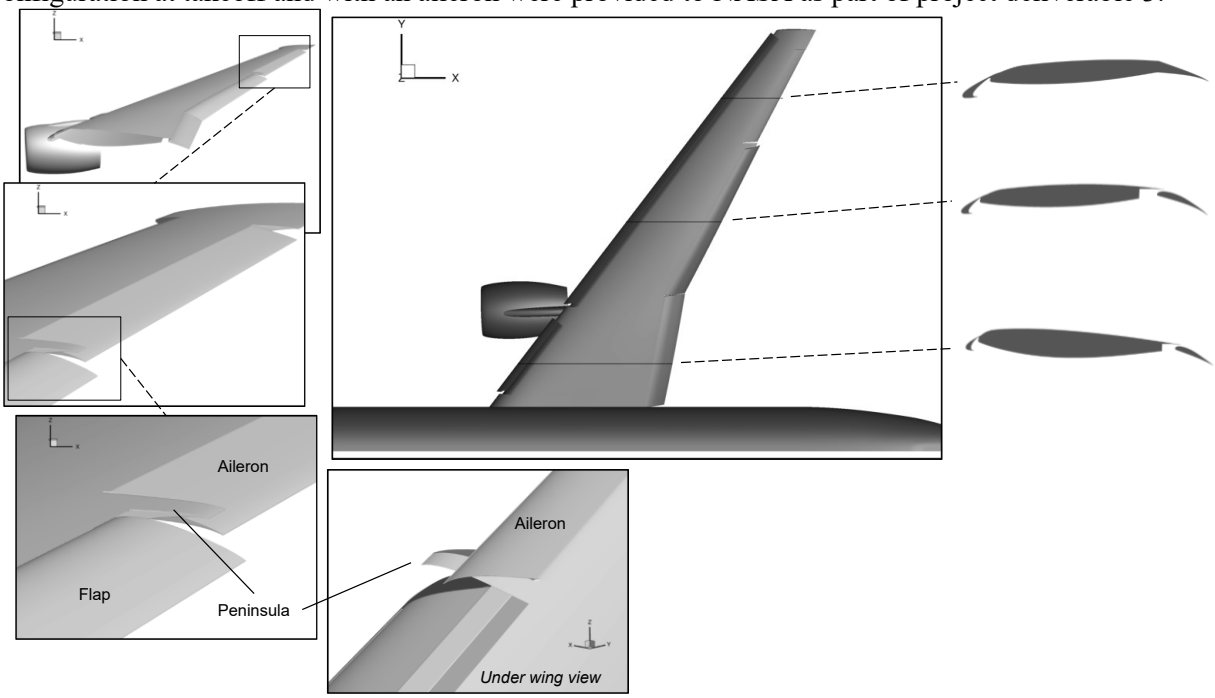

Figure 4 – CRM-HL wind tunnel surface definition for the aileron at 16°.

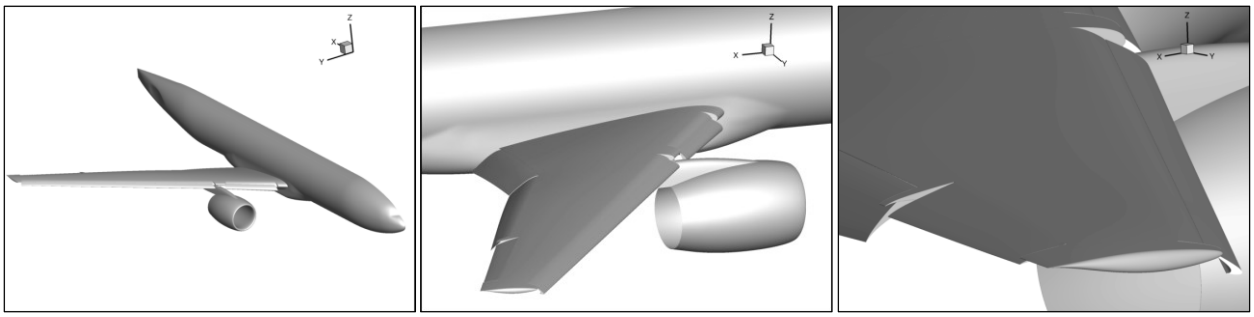

Figure 5 – CRM-HL surface definition with details of the sealed slat for takeoff.

2.2 Planform and AFC Scaling Between Reference Aircraft and CRM-HL

Guidelines for actuation layout and actuation parameters have been drawn from the experience gained from the CFD simulations on the Reference Geometry. First, the scaling between the Reference Aircraft and the CRM-HL model has to be determined. Here, it is important to point out that the two configurations represent different classes of commercial airplanes. The Reference Aircraft represents a short/medium range commercial airplane whereas the CRM-HL is representative of a long range commercial transport. The geometrical attributes of the two airplane types are illustrated in Figure 6, underscoring the different airplane sizes and wing sweep angles.

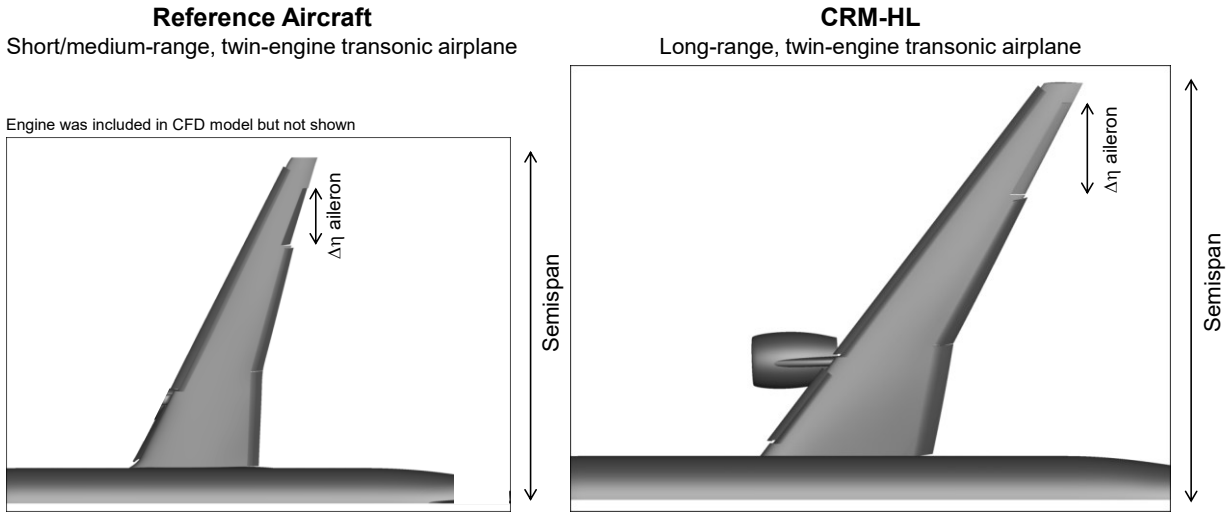

Figure 6 – Difference of the aileron AFC study between Reference Aircraft and CRM-HL.

The most important factor in establishing the AFC layout is the effective actuation area, which is the combined cross sectional area of the actuators, customarily defined at the throat sections. Here the actuator area is scaled by wing area ratios and aileron length ratio between the Reference Aircraft and the CRL-HL geometry. The actuators' area of the CRM-HL is 2.17 times larger than that of the Reference Aircraft. Two layout options are considered here, based on the results for the discrete nozzles (or ducts) and the blowing nozzle from the CFD report.

Figure 7 is an illustration of the scaling process from the Reference Aircraft to the CRM-HL for the discrete blowing nozzle system AR2 (final report document #2 [1], Section 4.1.4). The full-scale Reference Aircraft employs 78 actuators having a combined throat area of $0.5536in^2$. An equivalent actuation on the full-scale CRM-HL will require a total throat area of $1.2in^2$. In principle, the design could employ a different number of actuators, as long as the total throat area is preserved and the spacing between actuators is not too large. With respect to the wind tunnel model, the total throat area for the 10%-scale CRM-HL model translates to $0.012in^2$. Based on these estimates, for example, a supply of PR=3.5 is expected to provide a

3% increase in L/D. Clearly the size of these actuators poses challenges with regard to the design and manufacturability of the model, which will be addressed further in Section 4.

Full scale				
	units	Ref Aircraft	CRM	notes
Scale factor		2.17		CRM/RefG
Actuator options				
1 - Discrete CD ducts				per CFD Report, Secion 4.1.4
Throat dim (h/w)	in	0.0596x0.119		
AR		2		Small AR may be less efficient
#		78		
Athroat/actuator	in2	0.0071		
Total Athroat	in2	0.5538	1.20	This is FS total area needed for CRM
Model scale (10%)	in2		0.012	This is WT total area needed for CRM

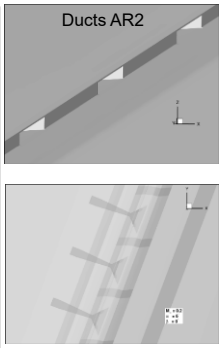

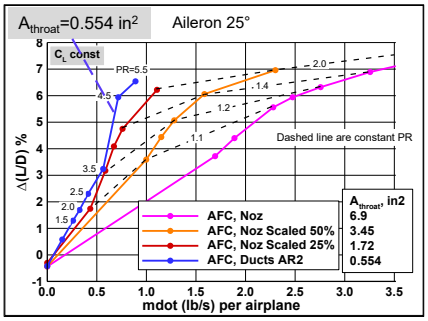

Reference Aircraft – Discrete Ducts
(CFD Report, Sec 4.1.4)

Figure 7 – AFC layout on the CRM-HL based on discrete ducts per the analysis on the Reference Aircraft.

Full scale				
	units	RefG	CRM	ratio (CRM/RefG)
Scale factor				2.17
Actuator options				
2 - Elongated nozzle				Per CFD Report, Section 4.1.3
#		1		
Athroat/actuator	in2	3.45		
Total Athroat	in2	3.45	7.48	This is FS total area needed for CRM
Model scale (10%)	in2		0.075	This is WT total area needed for CRM

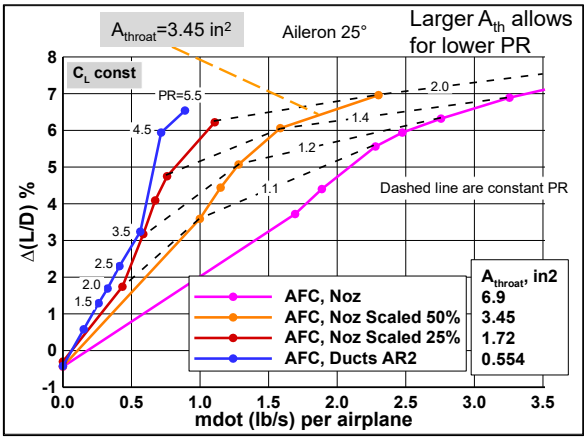

Reference Aircraft – Blowing nozzle
(CFD Report, Sec. 4.1.3)

Figure 8 – AFC layout on the CRM-HL based on the blowing nozzle per the analysis on the Reference Aircraft.

Figure 8 shows the scaling performed for the AFC layout based on the blowing nozzle 50% (final report document #2 [1], Section 4.1.3). The nozzle throat area on the Reference Aircraft is 3.45in^2, which translates to 7.48in^2 on the CRM-HL, or 0.075in^2 on the 10%-scale model. Relative to the discrete nozzles, for the same actuation effect, the larger actuation area will require lower actuation pressure. This can be clearly inferred from the insets in Figures 7 and 8 that show the gains in L/D versus actuation input. These trends are instrumental in establishing trades between PR and mass flow to identify the best candidate that could practically accommodate the supply at the wind tunnel facility and an actuator size that can be manufactured.

It is noted that although most of the CFD results in Figures 7 and 8 were obtained for the blowing nozzle, they can be used as proxy for an equivalent discrete ducts layout and with other nozzles types.

3 Numerical Results

The CFD evaluation of AFC applied at the aileron of the CRM-HL is described in this section. The implementation draws by and large from the experience gained from the study of the Reference Airplane. Subsequently, a conceptual design for the wind tunnel model is presented, while considering the available fluidic resources at the test facility. The actuation for the CRM-HL is based on the blowing nozzle 50% discussed in the final report document #2 [1], Section 4.1.3. The scaling and layout of this actuation was described in Section 2.2 as it relates to Figure 8.

3.1 Baseline Flow at Takeoff

The first set of results is used to gain insight into the flow development as a function of aileron deflection for the baseline unactuated flow. The aileron is deflected at 0°, 7.5°, 16° and 25°, where 7.5° is considered the nominal angle for takeoff (also dubbed nominal aileron), against which performance improvements will be measured. The freestream Mach number is 0.20 and Re=6 million, consistent with the conditions anticipated at the 14x22 facility. The nominal angle of attack at takeoff is 8°.

Figure 9 shows the flow field for the 7.5° aileron deflection at α=8° in terms of surface pressure distributions, regions of flow separation (in gray), and the normalized total pressure PT at a set of cross sectional cuts downstream of the wing. The pressure contours selected wing cuts are also presented. Figure 10 shows the flow fields for the 0°, 7.5°, 16° and 25° aileron deflection angles. The flow is fully attached on the undeflected aileron, but progressively larger separation forms at increasingly higher angles, triggered by the adverse pressure gradient close to the hingeline. At the nominal deflection, the flow is separated at the trailing edge of the aileron. However, at the 25° deflection, the flow over the aileron is separated over nearly the entire span, indicating a thicker wake with larger total pressure loss. This is also evident from the total pressure contours at the midaileron cross-sections, where the black lines denote the regions of flow reversal. This is indicative of higher drag. The total pressure also indicates that the tip vortex elements get stronger, commensurate with the increased aileron loading at the largest deflection. The tip vortex from the inboard edge of the aileron is particularly coherent.

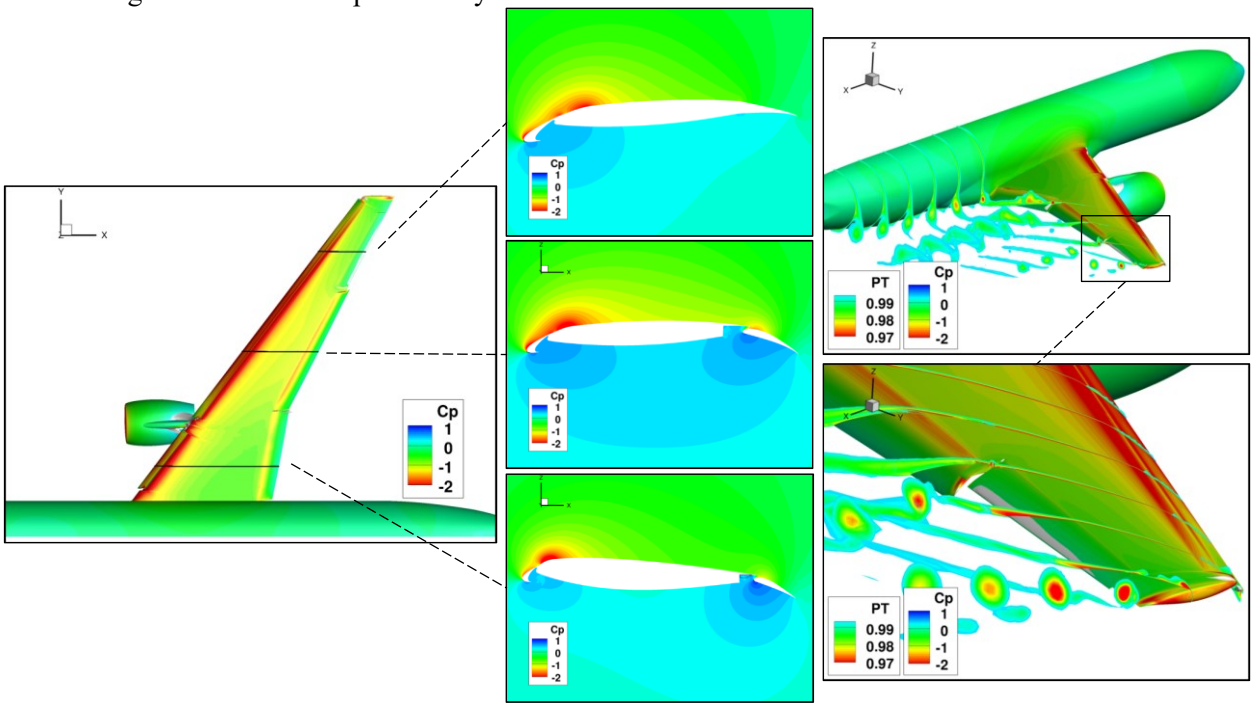

Figure 9 – Baseline flow for the nominal takeoff condition of 8° and nominal aileron deflection of 7.5°.

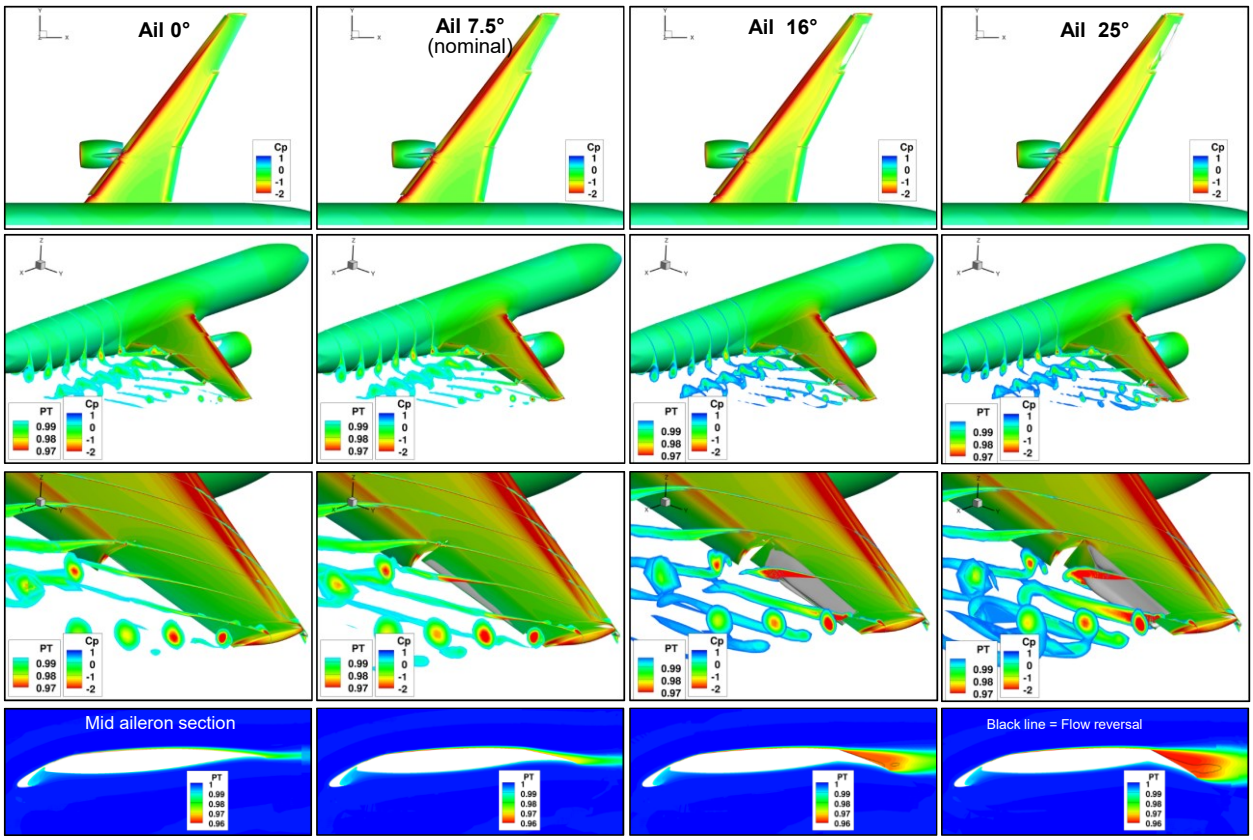

Figure 10 – Baseline flows fields for the different aileron deflections at the nominal takeoff condition (α=8°).

Turning now to the impact on aerodynamic characteristics, as the aileron is deflected, the increased wing camber results in increased global circulation affecting the entire wing section, and hence higher lift. As the aileron is deflected to higher angles, the flow starts to separate and drag becomes significant. This is clearly shown in the aerodynamic performance in Figure 11, where the drag increment at large deflections is such that L/D drops at around 10°. Here the dashed lines denote the nominal aileron deflection of 7.5°. The simulations indicate a peculiar trend at the angle of attack of 12°, with notable deficiency in lift. It is believed that this behavior is due to the absence of the nacelle chine in the current CFD model, as this anomaly has been observed in another study as well [6]. It is noted that the nacelle chine was incorporated in the CFD model of the Reference Airplane, and hence this peculiar behavior was not detected. Nevertheless, the overall trends in Figure 11 indicate that this problem should not detract from the current flow control study and the eventual inclusion of the chine should resolve this issue. The goal here is to augment L/D beyond the level achieved with the nominal aileron deflection by using a larger aileron deflection in conjunction with flow control. Specifically, AFC will be used to lower the pressure drag by reducing flow separation, and the induced drag through spanload redistribution.

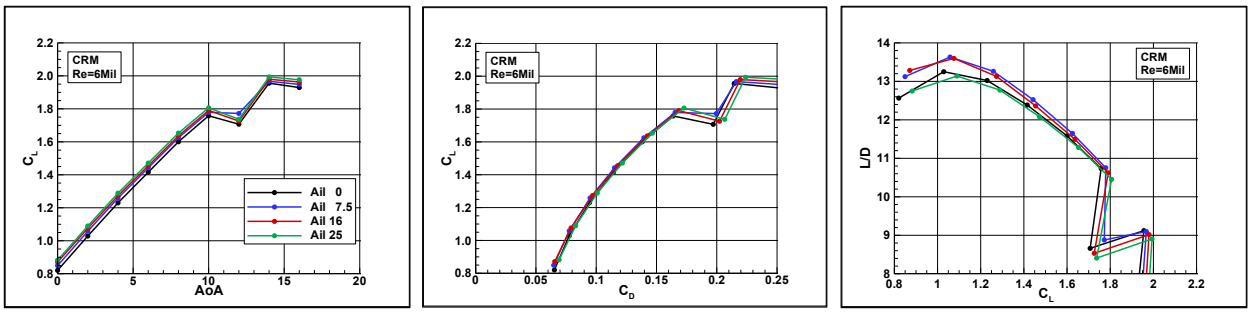

(a) Aerodynamic characteristics along the range of angles of attack

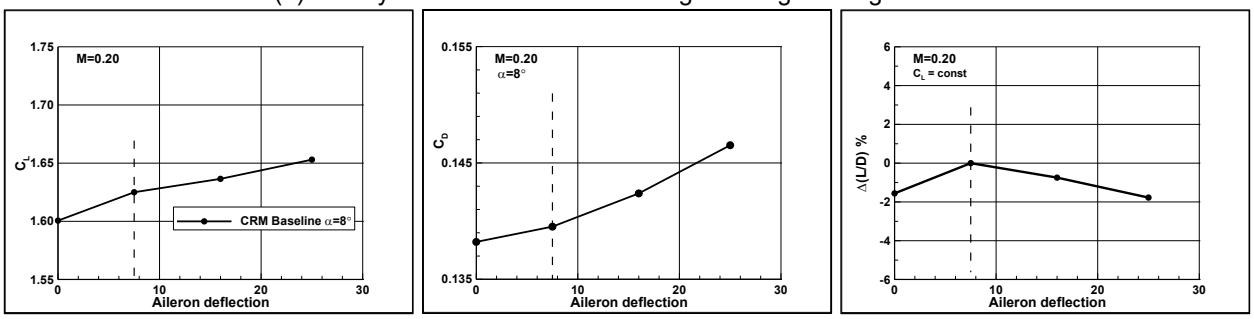

(b) Aerodynamic characteristics at α=8°as function of aileron deflection

Figure 11 – Baseline flow: aerodynamic performance as function of aileron deflection.

3.2 AFC on the Deflected Aileron

The flow control approach consists of a continuous nozzle that runs the full span of the aileron. This is essentially a two-dimensional convergent-divergent (CD) nozzle section in the vertical plane whose exit section forms a long slot along the aileron. The inlet consists of a constant area duct that is connected to a convergent duct section. The diffuser is long enough to ensure that its half angle is smaller than 15° to prevent the flow from separating. The nozzle cross section is identical along the span. This geometry was derived from the nozzle 50% used in the Reference Aircraft (final report document #2 [1], Section 4.1.3). Flow control was applied to ailerons 16° and 25°. The solutions for PR=2 are shown in Figures 12 and 13 for the 16° aileron deflection, and it is compared with the respective unactuated case, and also to the nominal aileron for reference.

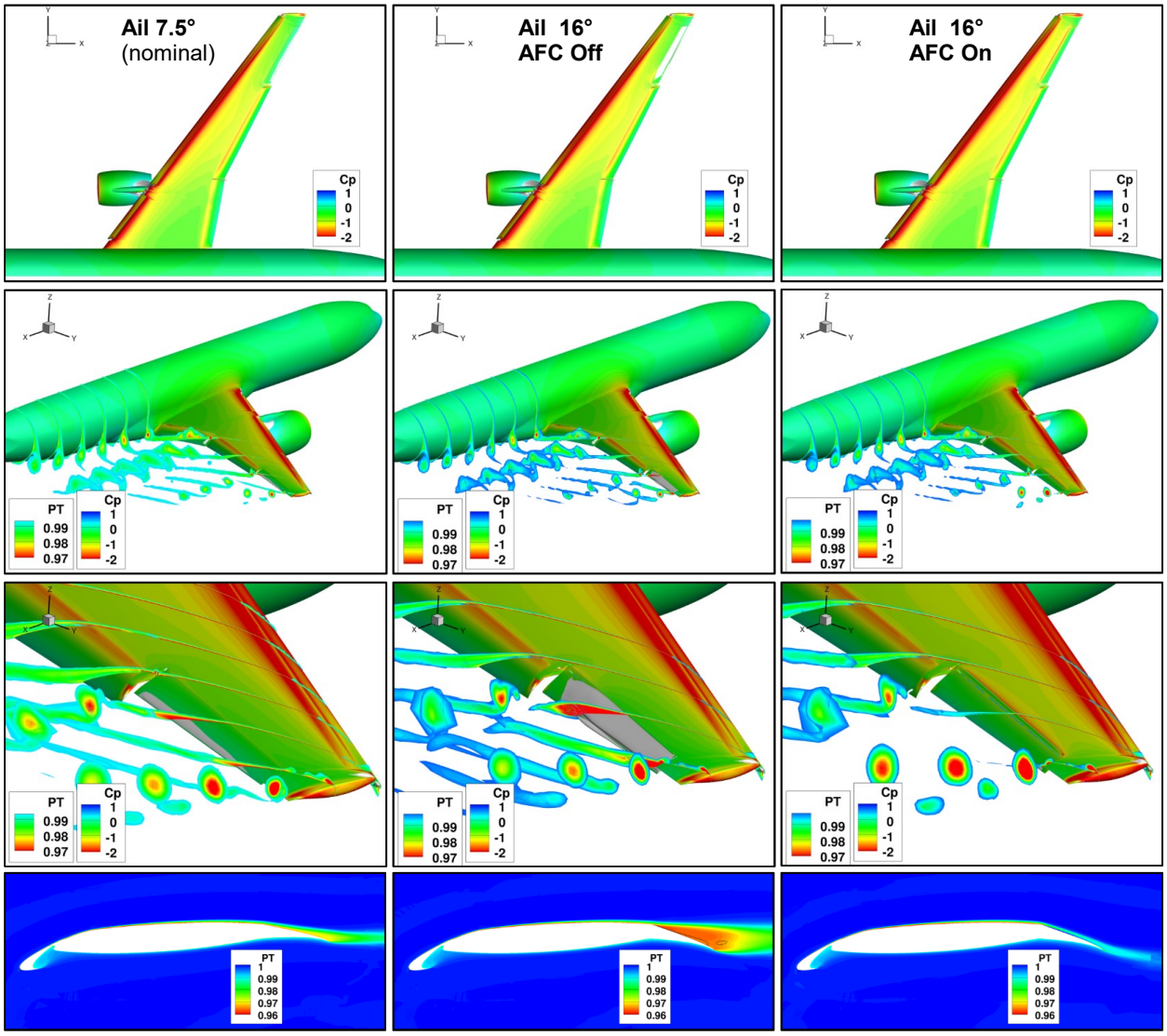

Figure 12 – Flows fields for the nominal aileron 7.5°, and aileron 16° with AFC off and AFC on (α=8°).

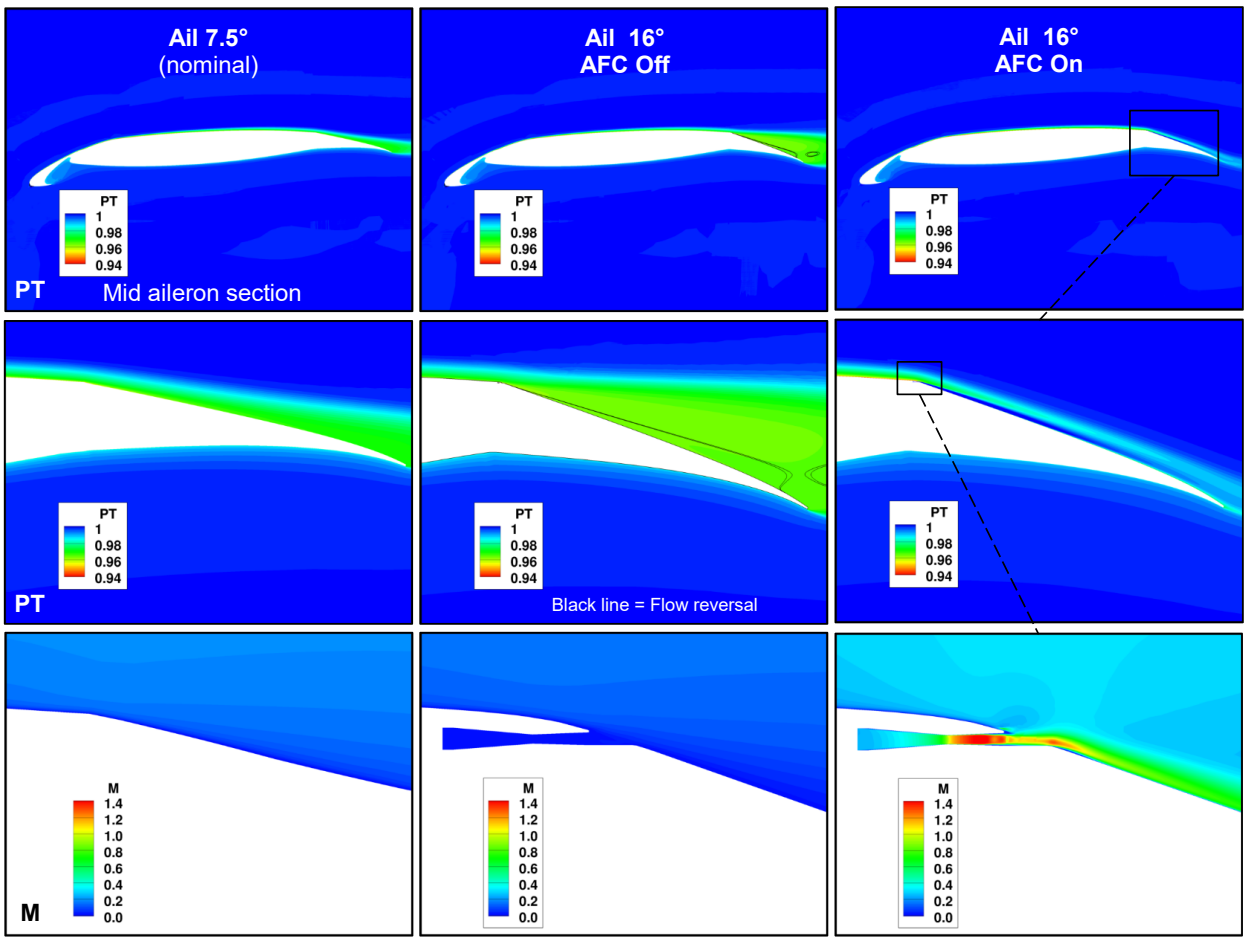

Figure 13 – Flows fields at the midaileron section for the cases in Figure 12.

The actuation is very effective in eliminating the flow separation. The intensity of the vortex sheet off the aileron has been considerably reduced. The vortex emanating from the outboard edge of the aileron is stronger relative to the unactuated case and it is the result of the increased loading on the aileron. The total pressure contours at the midaileron section in Figure 13 shows that the blowing jet affects the flow upstream of the hingeline, where the thickness of the viscous layer is reduced. At this pressure ratio, the CD nozzle becomes choked. The flow accelerates in the diffuser and the jet is ejected at supersonic velocity over the aileron. At this condition, the blanket of high speed flow helps energize the viscous layer and prevent flow separation over the entire aileron. The impact of AFC on the aerodynamic performance is shown in Figure 14. Flow control results in increased lift over the lift range, including $C_{L,max}$. Additionally, the reduced separation results in lower drag. The combined effects result in significantly higher L/D.

The aerodynamic performance as a function of actuation mass flow coefficient C_q is also included in Figure 14. The lift is obtained at α=6° and the percentage increment in L/D due to AFC taken relative to the corresponding baseline C_L. The baseline (unactuated) aileron 16 results in higher lift relative to the nominal aileron, but it comes with higher drag, as indicated by the drop of about 1% in L/D. However, flow control makes up for this shortfall with a very small pressure ratio. As input pressure becomes larger, the incremental lift and L/D become substantial. It should be noted that the C_q is small since it is being referenced to the wing area and it represents actuation input for both airplane ailerons.

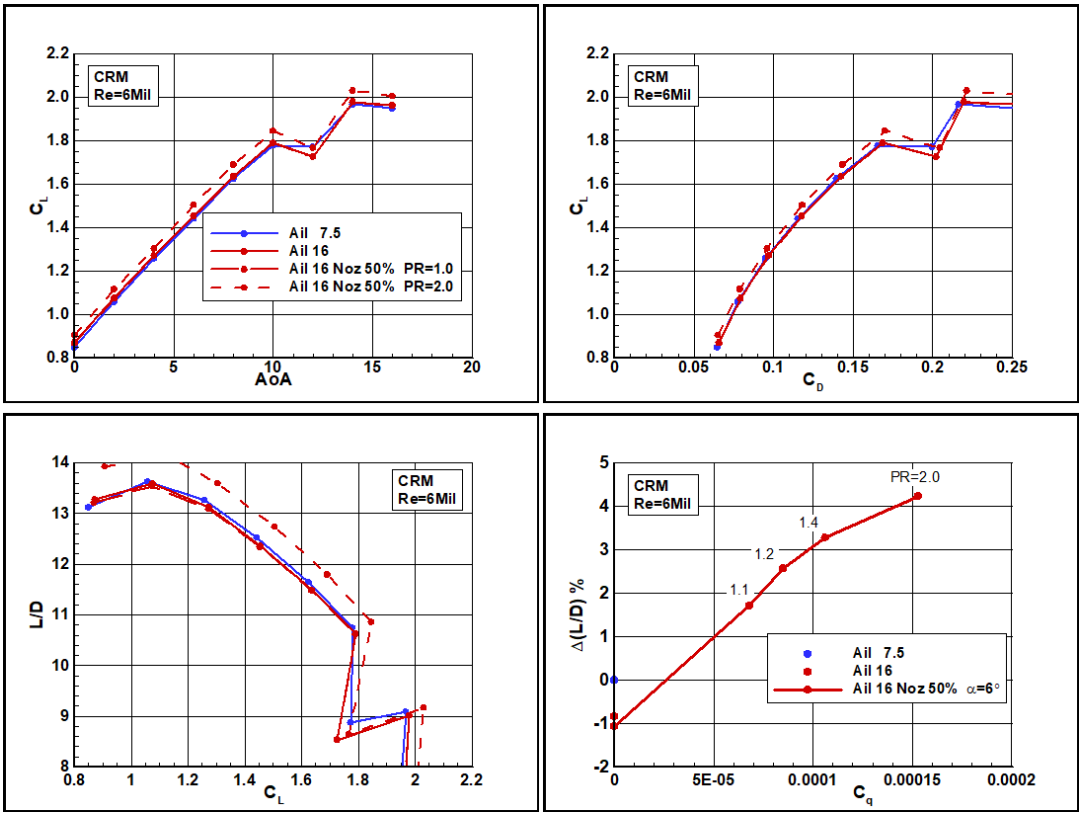

Figure 14 – Aerodynamic performance improvement due to AFC applied to aileron 16°.

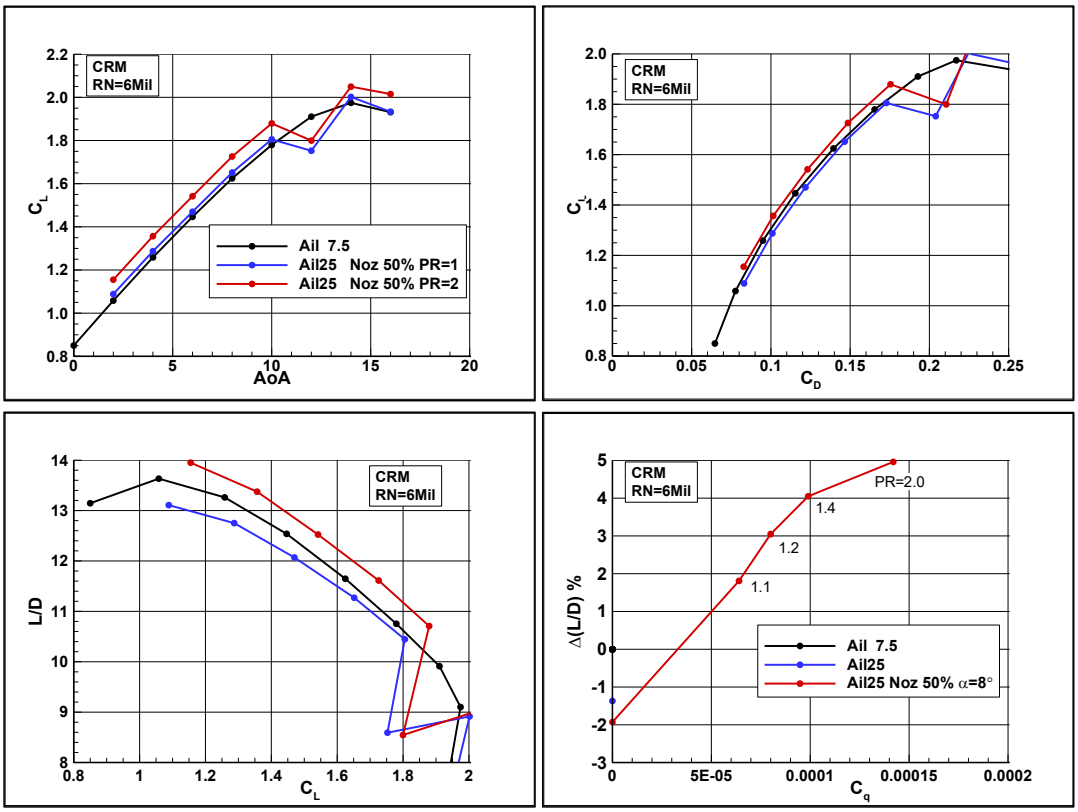

Figure 15 – Aerodynamic performance improvement due to AFC applied to aileron 25°.

Figure 15 shows the aerodynamic performance due to actuation on aileron 25°, demonstrating similar effects. The aerodynamic characteristics as a function of aileron deflection are summarized in Figure 16, quantifying the gains anticipated for different supply pressure ratios.

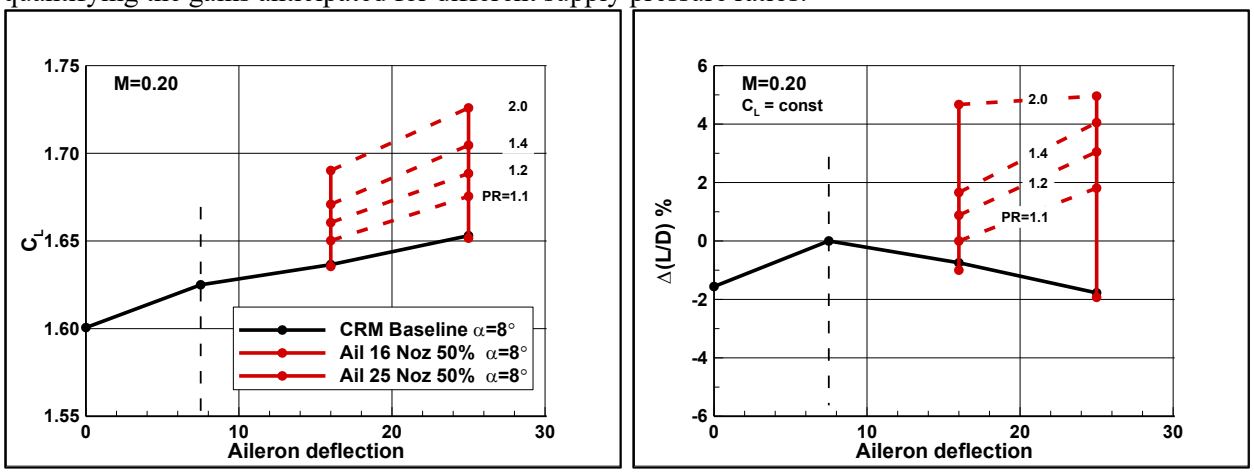

Figure 16 – Aerodynamic performance due to AFC using nozzle 50% as function of aileron deflection, α=8°.

4 Conceptual Modifications to NASA's CRM-HL Wind Tunnel Model

One of the tasks for the Boeing team was to provide conceptual designs for the modifications to NASA's CRM-HL wind tunnel model. An isometric view of the CAD model provided by NASA is illustrated in Figure 17. This model provided the basis for Boeing's conceptual designs. Generally, the team sought to develop a design concept that is as simple as possible while offering modularity for efficient model changes and wind tunnel testing. Also, the aileron unit was designed for ease of integration into the existing wind tunnel model without having to alter or sacrifice any existing structural elements. Due to the scale and tolerances required, all parts are conceptualized for machined metal to show the feasibility of the concept. However, the design can be adapted to 3D printing during the detailed design if desired. Note that all design files and additional documentation were provided to the NASA team as part of Deliverable 7.

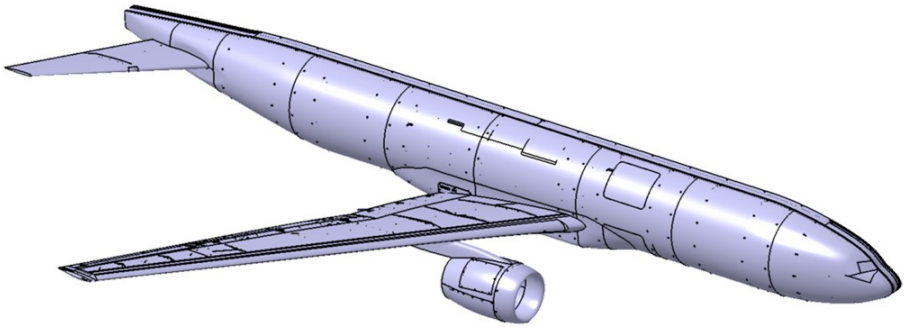

Figure 17 – CAD Model of the NASA CRM-HL wind tunnel model as received by the Boeing team.

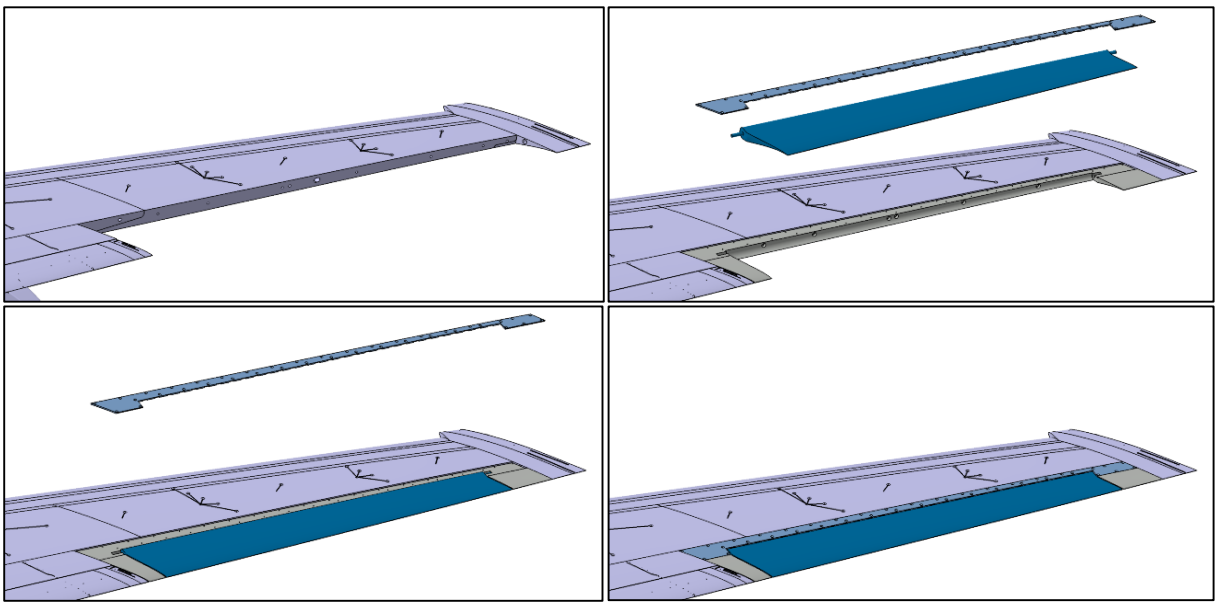

Figure 18 – Integration and assembly steps of aileron unit into CRM-HL wind tunnel model.

The wind tunnel model already has an outboard section that is removable without having to cut into any existing parts. The outboard portion of the wing with this section removed is depicted in the top left of Figure 18. Based on the aileron definition from Section 2.1, a new three piece insert was designed, which features the aileron as one of the components. Figure 18 shows the integration and assembly of the new aileron unit. A mounting frame is positioned within the opening of the outboard wing section (top right in Figure 18) which uses 6 existing threaded holes in the wing element for attachment with common hardware. This mounting frame houses the aileron where it can be held in place at various deflection angles (bottom

left in Figure 18). The aileron unit is completed by a cover plate that ensures a smooth continuation of the outer mold line (OML) between the main wing element and the aileron (bottom right in Figure 18). The cover plate is attached with common countersunk #2 screws. The AFC actuators are integrated in the cover plate. This modularity allows to easily reconfigure the AFC concept. Figure 19 illustrates an enlarged view of the three components that make up the aileron unit.

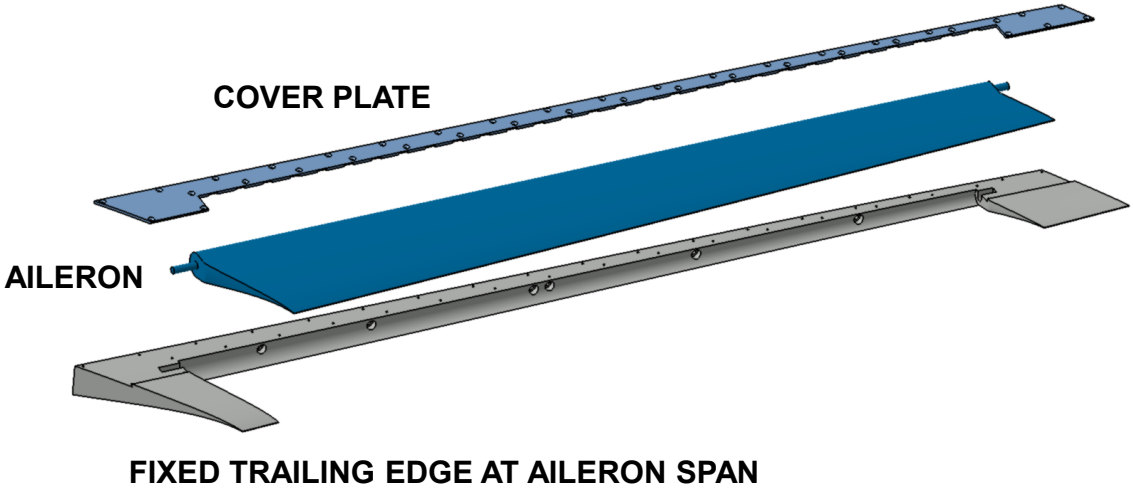

Figure 19 – Exploded view of aileron insert for CRM-HL wind tunnel model.

One of the important design considerations involves the setting of the aileron deflection angle. The design space ranges from continuous to predefined deflection settings. Furthermore, the aileron element can be deflected over a hinge or the OML can be designed to represent a deflected aileron. Within this design space, the number of required parts and the manufacturing effort have to be balanced with wind tunnel testing efficiency and number of possible configuration settings. For this conceptual design phase, the trade resulted in a design that features a deflection of an aileron. The deflection angle is set with shim elements between the cover plate and aileron hinge shaft (Figure 20). These shims are small, simple and reconfigurable parts that can be easily manufactured and replaced during testing. The aileron angle can be set accurately and repeatedly. Other concepts are possible to achieve similar results. Typically, the accurate setting and holding of a deflection angle can be involved and even costly in terms of manufacturing and part count.

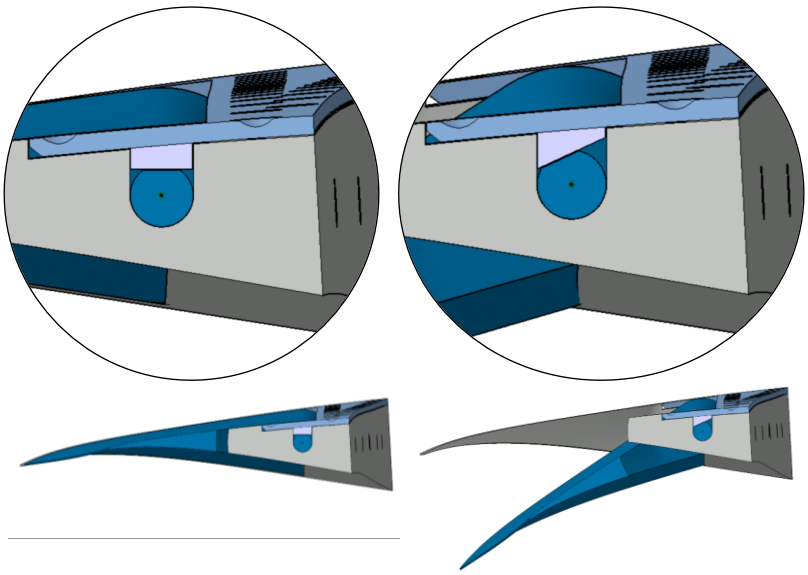

Figure 20 – Replaceable shim elements to set aileron deflection angles.

One of the potential AFC actuator configurations is conceptualized in Figure 21. The cover plate has 78 CD nozzles with an aspect ratio of width/height=2 implemented over approximately 30'' of hingeline. The exit angle of the jets is close to tangential to the local OML. The number and type of AFC actuators can be easily altered with separate cover plates. Furthermore, the spacing can be adjusted by blocking the convergent channel of every other or every third nozzle as desired. The cover plate can be manufactured with conventional machining and any AFC configuration can be prepared prior to a wind tunnel test. If the cover plate is left sufficiently thick in the design, it will also allow for adjusting the actuator height and exit angle. The CFD report in document #2 [1] presented the results of various AFC nozzle shapes and sizes, which concluded that the momentum coefficient is a leading parameter for the effects of AFC. With that in mind, the same momentum coefficient can be accomplished with different combinations of total nozzle exit area, supply pressure, and mass flow. This basis provides a convenient design space to tailor the actuator sizing to the available space on the wind tunnel model, and to account for potential supply pressure and mass flow limitations. For example, the cover plate may feature a dense array of small nozzles or a sparser array of larger nozzles to achieve the same total exit area. Also, a larger total exit area may be desirable if the supply pressure is limited while having sufficient mass flow available.

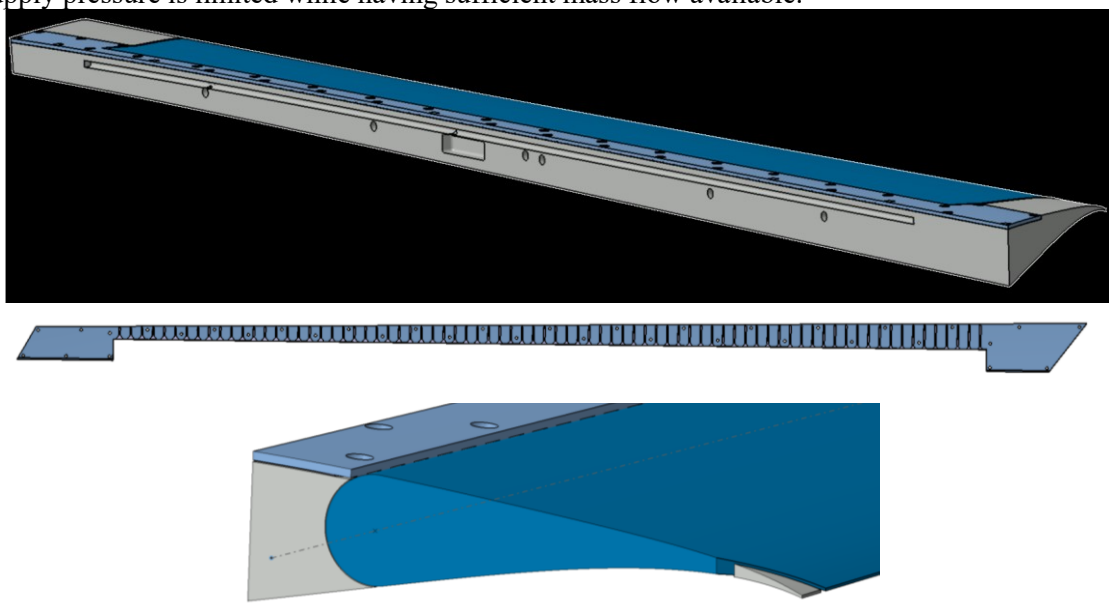

Figure 21 – AFC actuator integration angle and flow path.

The routing of air to the AFC actuators is another typical design challenge. Figure 21 indicates some potential solutions. An existing opening at the center of the rear face of the main wing element (visible in top left image of Figure 18) can be used to supply air to the aileron unit. The aileron mounting frame has a manifold of chambers and channels to distribute the air along the span of the aileron. Then the air is supplied from underneath the cover plate into the AFC nozzles either through discrete openings or a continuous channel. Note that some level of back pressure from the opening into the cover plate is desirable to achieve an even air distribution along the aileron span.

5 Conclusions and Future Work

This report concludes the fourth document of the final report package for the NASA/Boeing project on "Low-Speed Performance Enhancement using Localized Active Flow Control". The presented work is dedicated to the assessment of AFC over a deflected aileron on the CRM-HL model in order to support the preparation of a NASA wind tunnel test in January of 2023. As a first step, the differences between the Reference Aircraft (used in documents #2 [1] and #3 [2]) and CRM-HL are highlighted, as these planforms represent different airplane classes. The CRM-HL has a larger leading edge sweep angle and a larger planform area, which also results in relative differences of the aileron size. Because of these differences, the performance of AFC over the aileron in a takeoff configuration of the CRM-HL is found to be smaller relative to the Reference Aircraft. However, an increase in L/D of up to 5% is still accomplished with AFC when deflecting the aileron to 25° instead of the nominal 7.5°. This result also supports the scalability of AFC from the Reference Aircraft to the CRM-HL. If the actuation level is properly scaled to the size of the aileron on the CRM-HL, flow separation is successfully prevented when deflecting the aileron to higher angles. This scaling entails a design space that can be exploited to fit the requirements of the wind tunnel model in terms of available space for AFC integration, and potential limits on supply pressure and mass flow. The simulations presented in this report are based on scaled actuator sizing, which yielded similar aerodynamic capabilities at the same pressure ratio as for the Reference Aircraft.

In addition to the aerodynamic assessment with CFD simulations, conceptual designs are offered for the modification of the NASA 10% scale wind tunnel model of the CRM-HL. Generally, the wind tunnel model can be fitted with a new aileron insert without cutting or sacrificing any existing parts. The new insert features a mounting frame, an aileron element and a cover plate. The cover plate has the AFC actuators embedded. This modularity allows for the integration of any type of AFC actuator and provides flexibility in changing AFC parameters such as injection angle, spacing, nozzle size and nozzle aspect ratio. Furthermore, the model changes during wind tunnel testing can be accomplished quickly to maintain testing efficiency.

The planned test by NASA on their CRM-HL model will validate the numerical predictions of AFC performance on a deflected aileron. Furthermore, any validation on the CRM-HL model can also be transferred with reverse scaling to the simulations on the Reference Aircraft. The wind tunnel tests can confirm AFC scaling, in terms of actuator sizing and freestream velocity, and AFC optimization such as different AFC nozzles. During testing, various parameters such as angle of attack, aileron deflection angle, AFC actuation intensity, actuator spacing, etc. can be evaluated. The Boeing team can support the test preparation, execution and post-processing as needed. Furthermore, the Boeing team can review any additional CFD simulations that the NASA team may pursue in preparation of the wind tunnel test.

Despite the range of aspects addressed on the CRM-HL model, other topics remain unexplored. For example, the work on the Reference Aircraft suggests that localized AFC in the leading edge region of the wing where the flow interacts with the nacelle/pylon can significantly increase aerodynamic performance and potentially enable more efficient aircraft configurations. This concept can also be tested on the CRM-HL model.

References

1. Shmilovich, A., Vijgen, P., & Woszidlo, R., "Low-Speed Performance Enhancement using Localized Active Flow Control – Localized Active Flow Control Simulations on a Reference Aircraft", *NASA Technical Reports Server*, April, 2022, document ID: 20220006731
2. Vijgen, P., Ziebart, A., Shmilovich, A., & Woszidlo, R., "Low-Speed Performance Enhancement using Localized Active Flow Control – Integration Study of Localized Active Flow Control on a Performance Reference Aircraft", *NASA Technical Reports Server*, April, 2022, document ID: 20220006733
3. Lin, J.C., Pack Melton, L.G., Hannon, J., Andino, M.Y., Koklu, M., Paschal, K.C., & Vatsa, V.N., "Wind Tunnel Testing of Active Flow Control on the High Lift Common Research Model", *AIAA AVIATION Forum*, Dallas, TX, June 17-21, 2019, DOI: 10.2514/6.2019-3723
4. Lin, J.C., Pack Melton, L.G., Hannon, J., Andino, M.Y., Koklu, M., Paschal, K.C., & Vatsa, V.N., "Wind Tunnel Testing of High Efficiency Low Power (HELP) Actuation for Active Flow Control", *AIAA SciTech Forum*, Orlando, FL, Jan 6-10, 2020, DOI: 10.2514/6.2020-0783
5. Woszidlo, R., Shmilovich, A., & Vijgen, P., "Low-Speed Performance Enhancement using Localized Active Flow Control – Program Overview and Summary", *NASA Technical Reports Server*, April, 2022, document ID: 20220006728
6. Koklu, M., Lin, J.C., Hannon, J., Pack Melton, L.G., Andino, M.Y., Paschal, K.C., & Vatsa, V.N., "Investigation of the Nacelle/Pylon Vortex System on the High-Lift Common Research Model", *AIAA Journal*, Vol. 59, No. 9, Sept 2021, DOI: 10.2514/1.J059869